



## Determination of flood vulnerability level based on different numbers of indicators using AHP-GIS



I Gusti Agung Putu Eryani<sup>1\*</sup>, Made Widya Jayantari<sup>2</sup>, Suzana Ramli<sup>3</sup>

<sup>1</sup>Department of Civil Engineering, Warmadewa University, Indonesia

<sup>2</sup>Department of Civil Engineering, Udayana University, Indonesia

<sup>3</sup>School of Civil Engineering, Universiti Teknologi MARA, Malaysia

### Abstract

Vulnerability reduction and increased resilience are essential approaches to a flood management strategy. One of the most important steps is identifying flood-vulnerable areas. A flood vulnerability assessment is necessary to identify the areas. Currently, research on flood vulnerability assessment uses different indicators to determine the flood vulnerability level. However, it is unknown how the number of indicators used to assess flood vulnerability affects the results. This research aimed to determine the effect of the number of indicators used in estimating flood vulnerability using the AHP-GIS method on the resulting flood vulnerability level. Therefore, this research analyzed the weight of each indicator for five scenarios using the AHP method. This step is continued using GIS to create an overlay map to calculate each scenario's flood hazard index. The indicators used to determine the flood vulnerability index include elevation, slope, flow accumulation, drainage distance, land use, soil type, and annual rainfall intensity. The results showed that the reduction of indicators from seven to six caused the areas with moderate and very high levels of flood vulnerability to increase, while those with high levels decreased. Meanwhile, the reduction from six to five indicators caused the areas with low and moderate vulnerability to reduce, while those with high and very high levels increased. It was also discovered that when the indicators were changed from five to four, the areas with moderate and high vulnerability increased while those with very high levels decreased.

This is an open-access article under the [CC BY-SA](https://creativecommons.org/licenses/by-sa/4.0/) license.



### Keywords:

AHP;  
Flood;  
GIS;  
Vulnerability;

### Article History:

Received: April 6, 2023

Revised: Juli 19, 2023

Accepted: July 28, 2023

Published: February 2, 2024

### Corresponding Author:

I Gusti Agung Putu Eryani  
Department of Civil Engineering,  
Warmadewa University,  
Indonesia

Email: [eryaniagung@gmail.com](mailto:eryaniagung@gmail.com)

## INTRODUCTION

Global temperature is directly affected by the greenhouse effect caused by high carbon dioxide concentrations and other greenhouse gases in the atmosphere. Global warming will then cause an increase in evapotranspiration and atmospheric moisture content, causing changes in rainfall patterns [1][2].

These global climate changes will significantly affect the hydrological cycle and river flow regimes. Climate change is causing an increase in extreme weather. This condition causes an increase in the potential for hydrometeorological disasters, which have

significant implications for water resources, such as increased risk of flooding and erosion, decreased water quality, and further damage to ecosystems [3, 4, 5, 6].

Hydrometeorological disasters have occurred in almost all parts of the world. Indonesia is one of the countries in the world that was affected by this disaster. As much as 95% of the disaster trends in Indonesia are hydrometeorological disasters [7]. Flooding occurs when a river overflows its banks or the flood plains to the left and right of the river flow. The strength of rain dispersion to the soil, the amount of surface flow, and the strength of

erosion and flow capacity are all determined by the amount of rainfall, intensity, and distribution of rain [8, 9, 10]. Flooding has several negative impacts, such as damages to property and crops, disruption of transportation and utility services, and others associated with the disruption of economic activities or loss of human lives [7, 11, 12, 13].

Floods are expected to become more severe and frequent due to climate change, unplanned rapid urbanization, land use patterns, poor watershed management, and a decrease in groundwater recharge caused by the extension of impermeable surfaces in urban areas. Flood management is needed to protect people's safety, well-being, and the environment. Vulnerability reduction and increased resilience are essential approaches in a flood management strategy [14]. One of the most important steps in this strategy is identifying flood-vulnerable areas.

To identify flood-vulnerable areas, a flood vulnerability assessment is necessary. Flood vulnerability assessment quantitatively evaluates flood vulnerability using several indicators [15]. Currently, research on flood vulnerability assessment uses several indicators to determine the level of flood vulnerability. However, it is unknown how the number of indicators used to assess flood vulnerability affects the results [16, 17, 18].

Analytical Hierarchy Process (AHP) is a decision-making technique for multicriteria indicators, and the method has been applied to estimate different models [19]. The AHP method, combined with remote sensing techniques and geographic information systems (GIS), can be used to determine the level of flood vulnerability based on several indicators. Several indicators can be used to determine the flood vulnerability index, including elevation, slope, flow accumulation, drainage distance, land use, soil type, and annual rainfall intensity. The overlay method in GIS can be used to identify flood vulnerability quickly, easily, and accurately for mapping the flood vulnerability level [20, 21, 22, 23, 24].

This research aimed to determine the effect of the number of indicators used in estimating flood vulnerability using the AHP-GIS method on the resulting flood vulnerability level. Several scenarios with varying numbers of indicators are created. It is hoped that knowing how the number of indicators used affects the results of estimating flood vulnerability will be a reference for flood management stakeholders in choosing the number of indicators to use in

estimating the flood vulnerability level and the flood vulnerable area mapping.

## METHOD

### Research Area

Yeh Embang Watershed is located in Mendoyo District, Jembrana Regency covering an area of ± 61,561 Ha [25], as seen in Figure 1. The length of its river was 23 km [26]. Generally, the characteristics of rivers in the Province of Bali are divided into groups of rivers flowing north and rivers flowing south. Rivers flowing north are generally intermittent and short rivers, whereas those flowing south are permanent and longer rivers [27]. Based on precipitation data from 1993 to 2018, the Yeh Embang watershed's average annual precipitation is 2067 mm/year. Yeh Embang Village is the center of settlement or activity at a sub-district scale with several villages, development, and service directions due to its functions and potential [28], as seen in Figure 2 (a). Extreme flooding occurred in the Yeh Embang River Basin in 2018, 2020, and 2022, causing some damage to public facilities such as roads, bridges, and several houses, as seen in Figure 2 (b) [28][29].

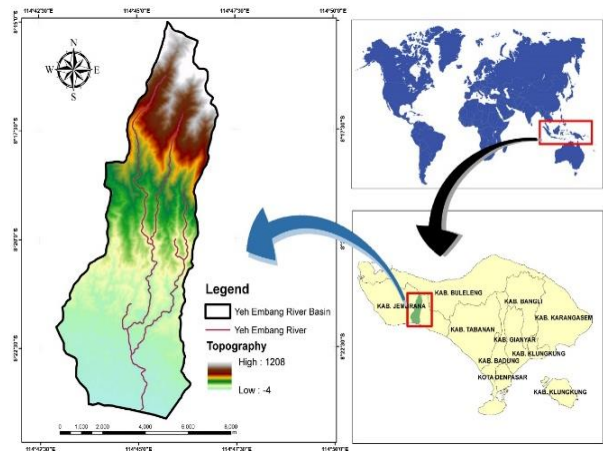


Figure 1. Research Location



Figure 2. Yeh Embang Watershed Normal Condition (a) and in Flood Condition (b)

## Research Data

Digital Elevation Model (DEM) data from the Yeh Embang watershed obtained from DEMNAS (<https://tanahair.indonesia.go.id/demnas/#/>) with 0.27-arcsecond spatial resolution determined using the EGM2008 vertical datum were used in this research.

The DEM data, as presented in Figure 3, was applied to analyze the flow accumulation, elevation, and slope. Rainfall data were obtained from the Poh Santen rainfall post (8°22'7.68" North Latitude and 114°40'20.22" East Longitude). The Bali-Penida River Basin Center obtained the rainfall data from 1993 to 2018. The soil type map was determined based on the digitization of the Bali Province Soil Type Map in 2018 from the Center for Environmental Research, Udayana University. The land use map was obtained from the Bali-Penida River Basin in 2018. Furthermore, the weight of each indicator used in the AHP analysis was obtained from previous studies from related journals.

## Methods

This research is initiated by identifying the problem. Flood vulnerability maps are essential for flood management. In previous flood vulnerability assessment research, the number of indicators used varied. However, no research has been conducted on the effect of the number of indicators used on the resulting level of flood vulnerability. This study aims to determine the different levels of flood vulnerability using various indicators. The result of this study is expected to be a consideration for further research to determine the number of indicators for flood vulnerability assessment. The data used in this study is a map of many indicators that will be overlaid using QGIS 3.10. Then a literature review was carried out from previous studies to obtain each indicator's priority level, and each indicator's weight was analyzed using the AHP method for each scenario.

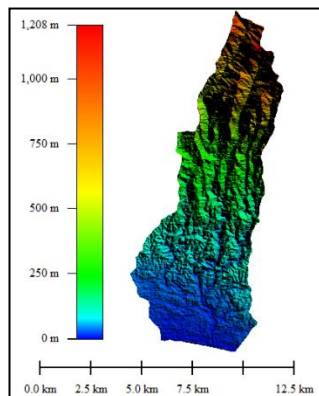


Figure 3. Yeh Embang Digital Elevation Model

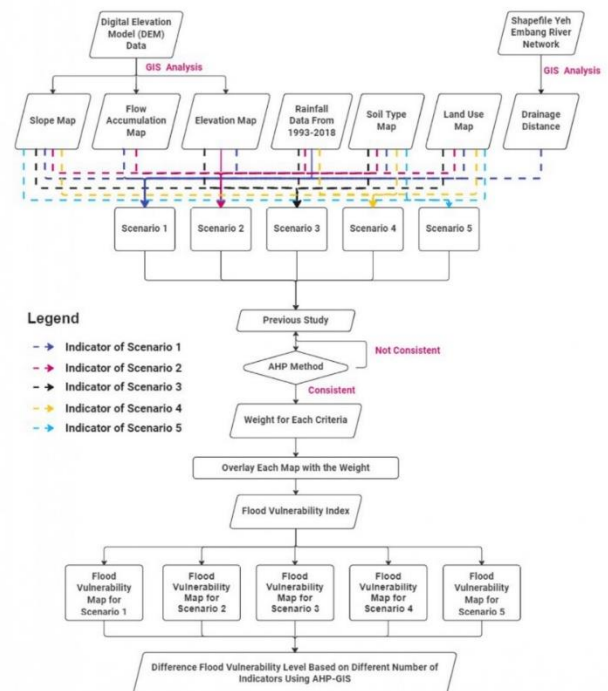


Figure 4. A Framework of the Research

Differences in flood vulnerability level will be seen for five scenarios with different indicators. Scenario 1 uses seven indicators, scenario 2 uses six indicators, scenario 3 uses five indicators, scenario 4 uses four, and scenario 5 uses three. The indicators used in each scenario can be seen in the framework diagram in Figure 4.

## Flood Vulnerability Index

The indicators used to determine the flood vulnerability index include elevation, slope, flow accumulation, drainage distance, land use, soil type, and annual rainfall intensity.

## Analytical Hierarchy Process (AHP)

The Analytical Hierarchy Process (AHP) is a measuring theory used to calculate ratio scales from paired comparisons that are both discrete and continuous. These comparisons can be made using objective measurements or a basic scale reflecting the relative strength of preferences and sentiments. To use the AHP to model an issue, a hierarchical or network structure must be used to describe the problem, and pairwise comparisons must be used to build relationships within the structure. Pairwise comparisons are essential when using the AHP. Members of parliament must first define priorities for their primary criteria by assessing their relative relevance in pairs, resulting in a pairwise comparison matrix [30].

## RESULTS AND DISCUSSION

### Rainfall Intensity

The annual rainfall data from the nearest rain post, Poh Santen, located at 8°22'7.68" latitude and 114°40'20.22" east longitude, were used due to the limited availability of rain stations around the Yeh Embang watershed. The data covers the daily rainfall from 1993 to 2018; each year's values were added to determine the average. The data were classified into different categories, including more than 2500 mm/year, 2000 – 2500 mm/year, 1500 – 2000 mm/year, 1000 – 1500 mm/year, and less than 1000 mm/year [31]. It is important to note that the existence of higher rainfall in an area usually leads to a more significant potential for flooding. It was discovered from the analysis that the average annual rainfall of the Yeh Embang watershed from 1993 to 2018 was 2067 mm/year.

### Flow Accumulation

Flow Accumulation is defined as the amount of water flowing in the river. The greater the flow accumulation value, the greater the potential for flooding. It was determined in this study through the Digital Elevation Model (DEM) analysis, and the findings showed that the value for the Yeh Embang watershed ranges from 0-651,203 pixels which were further classified into five classes with the same interval.

### Soil Type

The soil types also influence the determination of flood-vulnerable areas due to the differences in their infiltration properties. It is important to note that the soils with smaller or more difficult opportunities for water infiltration usually have a higher possibility of flooding. The soils used were divided into five classes which include Alluvial, Planosol, and Hydromorph; Latosol; Timberland and the Mediterranean; Andosol, Lateritic, Grumosol, and Podzol; and Regosol, Lithosol, Organosol, and Renzina [31].

### Elevation

Elevation defines the high and low of an area, with the lower part discovered to have a higher potential for flooding. This research determined the elevation using the digital elevation model (DEM) through the data obtained from DEMNAS and later classified into five classes with equal intervals based on height.

### Slope

The slope is the division between distance and difference in elevation. Moreover, a greater slope usually leads to a steeper area and vice versa. Sloping areas also have a higher potential

for flooding because the flow speed becomes slower, thereby allowing the slow wastage of water into the sea during an enormous discharge which subsequently causes flooding. This research classified the slope into five, which include 0-8%, 8-15%, 15-25%, 25-45%, and more than 45%.

### Land Use

Land use also greatly influences water infiltration, like the soil type. This condition occurs because land with higher usage usually makes it more difficult for water to infiltrate, increasing the vulnerability to flooding. This research divided land use into five classes: Residential, Rice fields/Agriculture Land, Field/Farm Shrubs, and Forest [31].

### Distance Drainage

The distance of the area to the river flow also affects the vulnerability to flooding. Therefore, the drainage distance indicator was divided into areas <200, 200-500 m, 500-1000 m, 1000-2000 m, and >2000 m to the river flow. It is important to note that the areas closer to water sources usually have higher vulnerability and vice versa.

### Weight of each Indicator

Several studies have estimated the level of flood vulnerability using different numbers of indicators [17]. However, no research has been conducted on the effect of the number of indicators used on the resulting level of flood vulnerability. This study aims to determine the different flood vulnerability levels using different indicators. Therefore, the AHP model was used to determine the weights for each indicator, after which QGIS software was applied to evaluate the flood vulnerability level through an overlay method.

The seven indicators were selected from the literature review. It was selected as the indicator frequently used in previous studies. Table 1 shows the relationship between the indicators. Rank 1 indicates weight greatly influencing flood vulnerability, while Rank 7 indicates the most minor influence.

Table 1 shows that the slope indicator is in the first Rank. This result means it was used in several studies as an indicator to estimate flood vulnerability. The result shows that the slope conditions' differences significantly influence flood vulnerability. Meanwhile, drainage distance is in the 7th Rank. Then it indicates that drainage distance is not widely used to estimate flood vulnerability. This ranking process was followed by determining the relationship between these indicators, as presented in Table 2.

Table 1. Indicator Ranking Based on Previous Research

Indicator Reference	Slope	Land Use	Soil Type	Rainfall Intensity	Elevation	Flow accumulation	Drainage Distance
Kazakis, Kougias and Patsialis [17]	6	4	7	5	2	1	3
Saini and S.P [32]	2	1	4	7	5	3	6
Vignesh et al. [33]	4	2	6	1	5	3	7
Dian et al. [34]	1	3	2	7	5	4	6
Ouma and Tateishi [16]	3	2	1	4	6	5	7
Eryani and Jayantari [35]	1	3	4	2	6	5	7
Hutauruk et al. [31]	1	4	2	6	3	5	7
Abdelkarim et al. [36]	3	6	7	4	5	2	1
Ardiansyah and Sumunar [37]	1	6	7	5	4	3	2
Desalegn and Mulu [23]	1	4	7	3	2	5	6
Kusmiyarti, Wiguna and Ratna Dewi [38]	1	3	4	2	5	6	7
Total	24	38	51	46	48	42	59
Rank	1	2	6	4	5	3	7

Table 2. Indicator Ranking Based on Previous Research

No	Indicator	Slope	Land Use	Soil Type	Rainfall Intensity	Elevation	Flow accumulation	Drainage Distance
[1]	[2]	[3]	[4]	[5]	[6]	[7]	[8]	[9]
1	Slope	1	2	6	4	5	3	7
2	Land Use	1/2	1	5	3	4	2	6
3	Soil Type	1/6	1/5	1	1/3	1/2	1/4	2
4	Rainfall Intensity	1/4	1/3	3	1	2	2	4
5	Elevation	1/5	1/4	2	1/2	1	1/3	3
6	Flow accumulation	1/3	1	4	2	3	1	5
7	Drainage Distance	1/7	1/6	1/2	1/4	1/3	1/5	1

The flood vulnerability indicator ranking results in Table 1 were used to develop the relationship between the indicators in Table 2. Score "6," placed in the first row of column [5], shows that the slope indicator is much more important than soil type. Furthermore, the score of "1/3" placed in row three of column [6] indicates rainfall intensity is more important than the soil type. These values were determined based on the results of previous related studies.

### Consistency Ratio

The Eigen factor was calculated for each scenario after the relationship between the indicators had been determined, as indicated in Table 3. This eigen factor was further used to evaluate the consistency ratio value for each number of indicators using formulas 1-2; the results are presented in Table 4.

$$CI = \frac{\lambda_{\max} - n}{n - 1} \quad (1)$$

$$CR = \frac{CI}{RI} \quad (2)$$

Where:

$\lambda_{\max}$  : Maximum eigenvalue of comparison matrix

n : Number of Indicators

C.R. : Consistency Ratio

CI : Consistency Index

R : Random Index

According to the AHP theory, an indicator can be declared consistent when the consistency ratio (C.R.) value is <0.1. The findings showed that the value for the seven indicators was 0.08, six indicators had 0.09, five indicators 0.03, four indicators 0.04, and three indicators 0.03. This result means all scenarios are consistent.

Table 3. Eigenvector matrix of the AHP

Number of Indicators	Eigenvector matrix of the AHP						
	Slope	Land Use	Soil Type	Rainfall Intensity	Elevation	Flow accumulation	Drainage Distance
7 Indicators	0.077	0.056	0.093	0.045	0.063	0.038	0.107
	0.386	0.449	0.279	0.361	0.316	0.342	0.250
	0.129	0.112	0.186	0.180	0.189	0.114	0.179
	0.055	0.037	0.023	0.023	0.021	0.023	0.036
	0.193	0.225	0.233	0.271	0.253	0.228	0.214
	0.064	0.045	0.047	0.030	0.032	0.028	0.071
	0.096	0.075	0.140	0.090	0.126	0.228	0.143
6 Indicators	0.082	0.058	0.095	0.046	0.065	0.039	
	0.408	0.467	0.286	0.369	0.323	0.350	
	0.136	0.117	0.190	0.185	0.194	0.117	
	0.204	0.233	0.238	0.277	0.258	0.233	
	0.068	0.047	0.048	0.031	0.032	0.029	
	0.102	0.078	0.143	0.092	0.129	0.233	
5 Indicators	0.094	0.066	0.118	0.057	0.080		
	0.472	0.529	0.353	0.453	0.400		
	0.236	0.264	0.294	0.340	0.320		
	0.079	0.053	0.059	0.038	0.040		
	0.118	0.088	0.176	0.113	0.160		
4 Indicators	0.522	0.566	0.400	0.480			
	0.261	0.283	0.333	0.360			
	0.087	0.057	0.067	0.040			
	0.130	0.094	0.200	0.120			
3 Indicators	0.600	0.625	0.500				
	0.300	0.313	0.417				
	0.100	0.063	0.083				

Table 4. Calculation of Consistency Ratio

Number of Indicators	$\lambda_{max}$	N	CI	RI	C.R.	Description
[1]	[2]	[3]	[4]= [2]-[3]/ [3]-1	[5]	[[6]=[4]/[5]	[7]
7	7.63	7	0.10	1.32	0.08	Consistent
6	6.56	6	0.11	1.24	0.09	Consistent
5	5.14	5	0.04	1.12	0.03	Consistent
4	4.11	4	0.04	0.9	0.04	Consistent
3	3.04	3	0.02	0.58	0.03	Consistent

**Flood Vulnerability Index (FVI)**

The weight for each indicator in each scenario was calculated. The criteria for each indicator are presented in Table 5. The formula used to calculate the FVI for seven indicators (scenario 1) which include Slope (S), Land Use (L), Soil Type (S.T.), Rainfall Intensity (R), Elevation (E), Flow Accumulation (F), and Drainage Distance (D) was  $FVI = 0.23 L + 0.05 ST + 0.34 S + 0.13 R + 0.07 E + 0.16 F + 0.03 D$ . The six indicators (scenario 2) which include Slope (S), Land Use (L), Soil Type (S.T.), Rainfall Intensity (R), Elevation (E), and Flow Accumulation (F)

used  $FVI = 0.24 L + 0.04 ST + 0.37 S + 0.13 R + 0.06 E + 0.16 F$ .

Moreover, the five indicators (scenario 3) with Slope (S), Land Use (L), Soil Type (S.T.), Rainfall Intensity (R), and Elevation (E) used  $FVI = 0.29 L + 0.05 ST + 0.44 S + 0.13 R + 0.08 E$ . The four indicators (scenario 4) with Slope (S), Land Use (L), Soil Type (S.T.), and Rainfall Intensity (R) used  $FVI = 0.31 L + 0.06 ST + 0.49 S + 0.14 R$  while the three indicators (scenario 5) with Slope (S), Land Use (L), and Soil Type (S.T.) obtained  $FVI = 0.34 L + 0.08 ST + 0.58 S$ .

Table 5. Weight for Each Indicator

Parameter	Class	Score	Weight				
			7 Indicators	6 Indicators	5 Indicators	4 Indicators	3 Indicators
Land Use	Residential	10					
	Rice fields/Agriculture	8					
	Land	6	0.23	0.24	0.29	0.31	0.34
	Field/Farm	4					
	Shrubs	2					
Soil Type	Forest	10					
	Alluvial, Planosol, Hidromorf	8					
	Latosol	6	0.05	0.04	0.05	0.06	0.08
	Timberland, Mediterranean	4					
	Andosol, Lateritic, Grumosol, Podzol	2					
Slope (%)	Regosol, Lithosol, Organosol, Renzina	10					
	0-8	8					
	8-15	6	0.34	0.37	0.44	0.49	0.58
	15-25	4					
	25-45	2					
Rainfall Intensity (mm/year)	>45	10					
	>2500	8					
	2000-2500	6	0.13	0.13	0.13	0.14	
	1500-2000	4					
	1000-1500	2					
Elevation	<1000	10					
	0 - 238.4	8					
	238.4 - 480.8	6	0.07	0.06	0.08		
	480.8 - 723.2	4					
	723.2 - 965.6	2					
Flow Accumulation (Pixel)	965.6 - 1208	10					
	520962.4 - 651203	8					
	390721.8 - 520962.4	6	0.16	0.16			
	260481.2 - 390721.8	4					
	130240.6 - 260481.2	2					
Distance from drainage network (m)	0 - 130240.6	10	0.03				
	<200	8					
	200-500	6					
	500-1000	4					
	1000-2000	2					
	>2000						

### Flood Vulnerability Map for Each Scenario

The flood vulnerability weight for each indicator in each scenario was used to calculate the flood vulnerability index, and the results are classified into very low, low, moderate, high, and very high. Scores range from 1 to 2 are classified as very low levels of vulnerability. Scores 2-4 are classified as low, scores 4-6 are classified as moderate, scores 6-8 are classified as high, and 8-10 are classified as very high. The map of the different levels of flood vulnerability for all the scenarios is presented in the following [Figure 5](#).

### Flood Vulnerable Level at Different Scenarios Based on AHP-GIS

The quantitative results obtained from mapping flood vulnerability levels for each scenario are presented in [Figure 5](#). According to the findings, when Scenario 1 is used, 19% of areas have low flood vulnerability levels, 44% moderate, 36% high, and 1% very high levels. In

Scenario 2, it indicates 19% for low, which is the same as the previous, 48% for moderate, which is a 4% increment, 28% for high, which is an 8% reduction, and 5% for very high, which is a 4% increase. Moreover, Scenario 3 produced a 15% low level, which is a 4% reduction from the previous scenario, a 36% moderate level, which is a 12% reduction, a 31% high level, which is a 3% increase, and an 18% very high level, which indicates a 13% increase. In scenario 4, 15% have a low level, which is the same as the previous scenario; 37% have a moderate level, indicating a 1% increase; 31% have a high level, which is the same; and 17% have a very high level, which is a 1% reduction. Meanwhile, Scenario 5 revealed that 33% of the areas have low flood vulnerability, an 18% increase over the previous scenario; 21% have a moderate vulnerability, a 16% decrease; 29% have a high vulnerability, a 2% decrease; and 17% have a very high vulnerability, the same as the previous scenario.

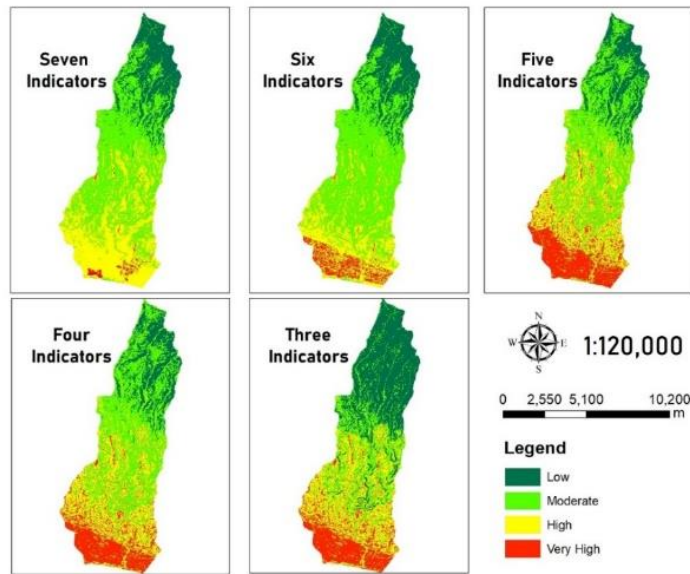


Figure 5. Flood Vulnerability Map for Each Scenario

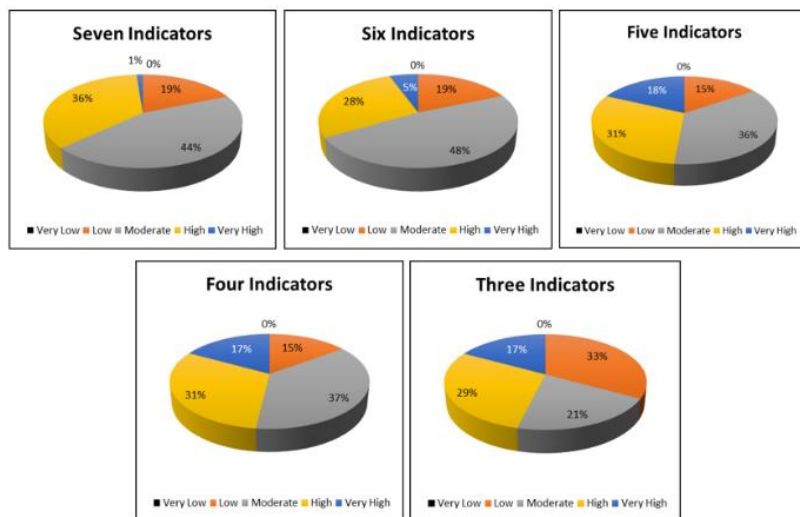


Figure 6 Differences in Flood Vulnerability Levels for Each Scenario

The analysis showed that the changes from the use of seven to three indicators caused the area with a low level of flood vulnerability to increase by 4%, the moderate level to decrease by 6%, the high level to reduce by 2%, and the very high level to increase by 2%. This result means the change in the number of indicators used in estimating flood vulnerability from three to seven does not provide a significant difference because the average difference is below 10%. The differences in flood vulnerability levels for each scenario can be seen in the pie chart in Figure 6.

**CONCLUSION**

The results showed that the reduction of indicators from seven to six caused the areas with

moderate and very high levels of flood vulnerability to increase, while those with high levels decreased. Meanwhile, the reduction from six to five indicators caused the areas with low and moderate vulnerability to reduce, while those with high and very high levels increased. It was also discovered that when the indicators were changed from five to four, the areas with moderate and high vulnerability increased while those with very high levels decreased. Moreover, the reduction from four to three indicators led to an increase in the areas with low flood vulnerability levels, while those with moderate and high levels decreased.

**ACKNOWLEDGMENT**

The authors appreciate Warmadewa University and Udayana University for their



support, Bali-Penida River Basin Center for providing data, and other parties that assisted in completing this research.

## REFERENCES

- [1] P. Blanco-Gómez, P. Jimeno-Sáez, J. Senent-Aparicio, and J. Pérez-Sánchez, "Impact of climate change on water balance components and droughts in the Guajoyo River Basin (El Salvador)," *Water (Switzerland)*, vol. 11, no. 11, 2019, doi: 10.3390/w11112360.
- [2] S. H. Pour, A. K. A. Wahab, S. Shahid, M. Asaduzzaman, and A. Dewan, "Low impact development techniques to mitigate the impacts of climate-change-induced urban floods: Current trends, issues and challenges," *Sustainable Cities and Society*, vol. 62, p. 102373, 2020, doi: 10.1016/j.scs.2020.102373.
- [3] L. Beevers, G. Walker, and A. Strathie, "A systems approach to flood vulnerability," *Civil Engineering and Environmental Systems*, vol. 33, no. 3, pp. 199–213, 2016, doi: 10.1080/10286608.2016.1202931.
- [4] K. M. Walters and M. Babbar-Sebens, "Using climate change scenarios to evaluate future effectiveness of potential wetlands in mitigating high flows in a Midwestern U.S. watershed," *Ecological Engineering*, vol. 89, pp. 80–102, 2016, doi: 10.1016/j.ecoleng.2016.01.014.
- [5] J. Qiu, Z. Shen, X. Hou, H. Xie, and G. Leng, "Evaluating the performance of conservation practices under climate change scenarios in the Miyun Reservoir Watershed, China," *Ecological Engineering*, vol. 143, no. November 2019, p. 105700, 2020, doi: 10.1016/j.ecoleng.2019.105700.
- [6] L. Mediero *et al.*, "Pluvial flooding: High-resolution stochastic hazard mapping in urban areas by using fast-processing DEM-based algorithms," *Journal of Hydrology*, vol. 608, no. February, 2022, doi: 10.1016/j.jhydrol.2022.127649.
- [7] A. Azmeri, H. Yunita, S. Safrida, I. Satria, and F. Z. Jemi, "Physical vulnerability to flood inundation: As the mitigation strategies design," *Journal of Water and Land Development*, vol. 46, no. 7–9, pp. 20–28, 2020, doi: 10.24425/jwld.2020.134194.
- [8] S. Adi, "Characterization of banjir bandang disasters in Indonesia," *Jurnal Sains dan Teknologi Indonesia*, vol. 15, no. 1, 2013.
- [9] R. Harini, B. Susilo, T. Sarastika, S. Supriyati, M. C. Satriagasa, and R. D. Ariani, "The Survival Strategy of Households Affected by Tidal Floods: The Cases of Two Villages in the Pekalongan Coastal Area," *Forum Geografi*, vol. 31, no. 1, pp. 163–175, 2017.
- [10] S. Hutapea, A. Maas, and R. Jayadi, "Biophysical Characteristics of Deli River Watershed to Know Potential Flooding in Medan City, Indonesia," *Journal of Rangeland Science*, vol. 10, no. 3, pp. 316–327, 2020.
- [11] S. Kheradmand, O. Seidou, D. Konte, and M. B. Barmou Batoure, "Evaluation of adaptation options to flood risk in a probabilistic framework," *Journal of Hydrology: Regional Studies*, vol. 19, no. March, pp. 1–16, 2018, doi: 10.1016/j.ejrh.2018.07.001.
- [12] S. Sharma, "Correlating soil and urban planning for sustainable water cycle," *Journal of Water and Land Development*, vol. 40, no. 1, pp. 137–148, 2019, doi: 10.2478/jwld-2019-0015.
- [13] B. W. Hastanti and F. J. Hutapea, "Analysis of Vulnerability Levels to the Flash Flood Based on Social Economic and Institutional Factors in Wasior, Teluk Wondama, West Papua," *Jurnal Wasian*, vol. 7, no. 1, pp. 25–38, 2020, doi: 10.20886/jwas.v7i1.4785.
- [14] N. Z. A. Norizan, N. Hassan, and M. M. Yusoff, "Strengthening flood resilient development in malaysia through integration of flood risk reduction measures in local plans," *Land use policy*, vol. 102, no. November 2020, p. 105178, 2021, doi: 10.1016/j.landusepol.2020.105178.
- [15] A. Díez-Herrero and J. Garrote, "Flood risk assessments: Applications and uncertainties," *Water (Switzerland)*, vol. 12, no. 8, pp. 1–11, 2020, doi: 10.3390/W12082096.
- [16] Y. O. Ouma and R. Tateishi, "Urban flood vulnerability and risk mapping using integrated multi-parametric AHP and GIS: Methodological overview and case study assessment," *Water (Switzerland)*, vol. 6, no. 6, pp. 1515–1545, 2014, doi: 10.3390/w6061515.
- [17] N. Kazakis, I. Kougiass, and T. Patsialis, "Assessment of flood hazard areas at a regional scale using an index-based approach and Analytical Hierarchy Process: Application in Rhodope-Evros region, Greece," *Science of The Total Environment*, vol. 538, no. December, pp. 555–563, 2015, doi: 10.1016/j.scitotenv.2015.08.055.
- [18] E. Feloni, I. Mousadis, and E. Baltas, "Flood vulnerability assessment using a GIS-based multi-criteria approach—The case of Attica region," *Journal Flood Risk Management*, vol. 13, no. S1, pp. 1–15, 2020, doi: 10.1111/jfr3.12563.
- [19] S. K. Sehra, Y. S. Brar, and N. Kaur, "Multi Criteria Decision Making Approach for Selecting Effort Estimation Model," *International Journal of Computers and Applications*, vol. 39, no. 1, pp. 10–17, 2012, doi: 10.5120/4783-6989.
- [20] S. Deepak, G. Rajan, and P. G. Jairaj, "Geospatial approach for assessment of vulnerability to flood in local self governments," *Geoenvironmental Disasters*, vol. 7, no. 1, 2020, doi: 10.1186/s40677-020-00172-w.
- [21] S. A. Ali *et al.*, "GIS-based comparative assessment of flood susceptibility mapping using hybrid multi-criteria decision-making approach, naïve Bayes tree, bivariate statistics and logistic regression: A case of Topla basin, Slovakia," *Ecological Indicators*, vol. 117, no. June, p. 106620, 2020, doi: 10.1016/j.ecolind.2020.106620.
- [22] S. A. Mohamed and M. E. El-Raey, "Vulnerability assessment for flash floods using GIS spatial modeling and remotely sensed data in El-Arish City, North Sinai, Egypt," *Natural Hazards*, vol. 102, no. 2, pp. 707–728, 2020, doi:

- 10.1007/s11069-019-03571-x.
- [23] H. Desalegn and A. Mulu, "Flood vulnerability assessment using GIS at Fetam watershed, upper Abbay basin, Ethiopia," *Heliyon*, vol. 7, no. 1, p. e05865, 2021, doi: 10.1016/j.heliyon.2020.e05865.
- [24] M. Jafari, R. Fazloula, M. Effati, and A. Jamali, "Providing a GIS-based framework for Run-Of-River hydropower site selection: a model based on sustainable development energy approach," *Civil Engineering and Environmental Systems*, vol. 38, no. 2, pp. 102–126, 2021, doi: 10.1080/10286608.2021.1893310.
- [25] Jembrana Regency Government, *Jembrana Regency Sanitation Report Book*. 2013. [Online]. Available: [http://ppsp.nawasis.info/dokumen/perencanaan/sanitasi/pokja/bp/kab.pasuruan/BAB III Sanitasi.pdf](http://ppsp.nawasis.info/dokumen/perencanaan/sanitasi/pokja/bp/kab.pasuruan/BAB%20III%20Sanitasi.pdf)
- [26] Central Bureau of Statistics of Bali Province, "River Names and Their Length by Regency/City in Bali Province," 2018. <https://bali.bps.go.id/statictable/2018/04/10/51/na-ma-nama-sungai-dan-panjang-menurut-kabupaten-kota-di-provinsi-bali.html>
- [27] R. Suyarto and T. Kusmawati, "Conditions and Problems of Water Resources and Agricultural Land in Bali Conditions and Problems of Water Resources and Agricultural Land in Bali," 2016.
- [28] S. Dharma, "Flash Flood on Yeh Embang River, Flooded Roads and Bridges," *Balipost.com*, Jembrana, Mar. 01, 2020. [Online]. Available: <https://www.balipost.com/news/2020/03/01/106998/Banjir-Bandang-di-Sungai-Yehembang,...html>
- [29] G. R. Warmadewa, "Broken Bridge, Isolated Residents of Sekar Kejula Kelod," <https://baliexpress.jawapos.com/>, Jembrana, Nov. 07, 2022. [Online]. Available: <https://baliexpress.jawapos.com/bali/17/10/2022/j-embatan-putus-warga-sekar-kejula-kelod-terisolir/>
- [30] R. W. Saaty, "The analytic hierarchy process-what it is and how it is used," *Mathematical model*, vol. 9, no. 3–5, pp. 161–176, 1987, doi: 10.1016/0270-0255(87)90473-8.
- [31] R. C. Hutauruk, S. Alfiandy, H. A. Nainggolan, and M. H. F. Y. Raharjo, "GIS-based Flood Susceptibility Mapping Using Overlay Method in Central Sulawesi," *Forum Geografi*, vol. 34, no. 2, pp. 136–145, 2020, doi: 10.23917/forgeo.v34i2.10667.
- [32] S. S. Saini and K. S.P, "Risk and vulnerability assessment of flood hazard in part of Ghaggar Basin: A case study of Guhla block , Kaithal , Haryana , India," *International Journal of Geomatics and Geosciences*, vol. 3, no. 1, pp. 42–54, 2012.
- [33] K. S. Vignesh, I. Anandakumar, R. Ranjan, and D. Borah, "Flood vulnerability assessment using an integrated approach of multi-criteria decision-making model and geospatial techniques," *Modeling Earth Systems and Environment*, vol. 7, no. 2, pp. 767–781, 2021, doi: 10.1007/s40808-020-00997-2.
- [34] R. Dian, L. Lismawaty, D. E. Pinem, and B. B. Sianipar, "Flood vulnerability and flood-prone area map at Medan City, Indonesia," *IOP Conference Series: Earth and Environmental Science*, vol. 200, no. 1, 2018, doi: 10.1088/1755-1315/200/1/012039.
- [35] I. G. A. P. Eryani and M. W. Jayantari, "Mapping of Flood Vulnerability and Mitigation Strategy of Unda River Basin Using Geographical Information System," 2021. doi: 10.9790/1813-1010015361.
- [36] A. Abdelkarim, S. S. Al-Alola, H. M. Alogayell, S. A. Mohamed, I. I. Alkadi, and I. Y. Ismail, "Integration of GIS-based multicriteria decision analysis and analytic hierarchy process to assess flood hazard on the Al-Shamal train Pathway in Al-Qurayyat Region, Kingdom of Saudi Arabia," *Water (Switzerland)*, vol. 12, no. 6, 2020, doi: 10.3390/W12061702.
- [37] A. Ardiansyah and D. R. S. Sumunar, "Flood Vulnerability Mapping Using Geographic Information System (GIS) in Gajah Wong Sub Watershed, Yogyakarta County Province," *Geosfera Indonesia*, vol. 5, no. 1, p. 47, 2020, doi: 10.19184/geosi.v5i1.9959.
- [38] T. B. Kusmiyarti, P. P. K. Wiguna, and N. K. R. Ratna Dewi, "Flood Risk Analysis in Denpasar City, Bali, Indonesia," *IOP Conference Series: Earth and Environmental Science*, vol. 123, no. 1, 2018, doi: 10.1088/1755-1315/123/1/012012.
- [39] A. N. Saputri and A. Witanti, "Coastal Vulnerability Classification of the North Coast of Java using K-Nearest Neighbor," *Journal of Integrated and Advanced Engineering (JIAE)*, vol. 3, no. 2, pp. 157-168, 2023, doi: 10.51662/jiae.v3i2.112